Next-generation sequencing analysis reveals that MTH-3, a novel curcuminoid derivative, suppresses the invasion of MDA-MB-231 triple-negative breast adenocarcinoma cells

YU-JEN CHIU[1-3], FUU-JEN TSAI[4,5], DA-TIAN BAU[6,7], LING-CHU CHANG[8], MIN-TSANG HSIEH[8,9], CHI-CHENG LU[10], SHENG-CHU KUO[8,9] and JAI-SING YANG[11]

[1]Division of Plastic and Reconstructive Surgery, Department of Surgery, Taipei Veterans General Hospital, Taipei 11217; [2]Department of Surgery, School of Medicine; [3]Institute of Clinical Medicine, National Yang Ming Chiao Tung University, Taipei 11221; [4]Human Genetic Center, China Medical University; [5]School of Chinese Medicine, China Medical University; [6]Department of Medical Research, China Medical University Hospital, China Medical University, Taichung 40402; [7]Department of Bioinformatics and Medical Engineering, Asia University, Taichung 41354; [8]Chinese Medicinal Research and Development Center, China Medical University Hospital; [9]School of Pharmacy, China Medical University; [10]Department of Sport Performance, National Taiwan University of Sport; [11]Department of Medical Research, China Medical University Hospital, China Medical University, Taichung 40402, Taiwan, R.O.C.

Received January 5, 2021; Accepted April 19, 2021

DOI: 10.3892/or.2021.8084

Abstract. Triple-negative breast cancer (TNBC) behaves aggressively in the invasive and metastatic states. Our research group recently developed a novel curcumin derivative, (1E,3Z,6E)-3-hydroxy-5-oxohepta-1,3,6-triene-1,7-diyl)bis(2-methoxy-4,1-phenylene)bis(3-hydroxy-2-hydroxymethyl)-2-methyl propanoate (MTH-3), and previous studies showed that MTH-3 inhibits TNBC proliferation and induces apoptosis *in vitro* and *in vivo* with a superior bioavailability and absorption than curcumin. In the present study, the effects of MTH-3 on TNBC cell invasion were examined using various assays and gelatin zymography, and western blot analysis. Treatment with MTH-3 inhibited MDA-MB-231 cell invasion and migration, as shown by Transwell assay, 3D spheroid invasion assay, and wound healing assay. The results of the gelatin zymography experiments revealed that MTH-3 decreased matrix metalloproteinase-9 activity. The potential signaling pathways were revealed by next-generation sequencing analysis, antibody microarray analysis and western blot analysis. In conclusion, the results of the present study show that, MTH-3 inhibited tumor cell invasion through the MAPK/ERK/AKT signaling pathway and cell cycle regulatory cascade, providing significant information about the potential molecular mechanisms of the effects of MTH-3 on TNBC.

Correspondence to: Dr Jai-Sing Yang, Department of Medical Research, China Medical University Hospital, China Medical University, No. 2, Yuh-Der Road, Taichung 40402, Taiwan, R.O.C
E-mail: jaisingyang@gmail.com

Dr Sheng-Chu Kuo, Chinese Medicinal Research and Development Center, China Medical University Hospital, No. 2, Yuh-Der Road, Taichung 40402, Taiwan, R.O.C
E-mail: sckuo@mail.cmu.edu.tw

Abbreviations: TNBC, triple-negative breast cancer; ER, estrogen receptor; GO, gene ontology; (HER2/neu), human epidermal growth factor receptor-2; PR, progesterone receptor; FBS, fetal bovine serum; DEGs, differentially expressed genes; KEGG, Kyoto Encyclopedia of Genes and Genomes; PI3K, phosphoinositide 3-kinase; RPKM, reads per kilobase per million mapped reads, p38/MAPK, mitogen-activated protein-serin kinase p38 α; MEK2, MAPK/ERK protein-serine kinase; PRAS40, proline-rich Akt substrate 40 kDa; CDC42, cell division control protein 42; CDK2, cyclin-dependent protein-serine kinase 2; ERK1/2, extracellular regulated protein-serine kinase 1 and 2, MMP, matrix metalloproteinase

Key words: curcuminoid derivative, triple-negative breast cancer (TNBC), anti-metastasis, MTH-3, next generation sequencing analysis

Introduction

Breast cancer is the most common primary cancer in woman, affecting approximately 12% of women worldwide (1). Breast cancer cases have markedly increased since the 1970s, which has been attributed to the modern lifestyle (2). There are various subtypes of breast cancer, including triple-negative breast cancer (TNBC), which lacks the expression of the genes encoding human epidermal growth factor receptor-2, progesterone receptor, as well as estrogen receptor. The majority of hormone and targeted therapies target one of the three aforementioned receptors, resulting in treatment resistance (2). In addition, TNBC is more common in young women, demonstrating relapse and aggressive behaviors during the invasive and metastatic states. Cancer relapse and distant metastasis

markedly increase morbidity and mortality, and are the most formidable obstacles to successful treatment (3). Current medical treatments, such as treatment with doxorubicin and toxoids, frequently lead to drug resistance and cause severe side effects (4). As a result, researchers are exploring novel treatment strategies for TNBC.

Natural products and their derivatives have recently become an important source of drug and therapeutic candidates (5). Between 1981 and 2010, approximately 34% of US Food and Drug Administration-approved novel-marketed drugs were derived from natural products (6). Curcumin, a golden color chemical derived from *Curcuma longa* plants, has been widely used in Traditional Chinese medicine in East Asia for centuries. Curcumin has diverse pharmacological properties, including anti-bacterial (7), anti-inflammatory (8), anti-oxidant (9), anti-depressant (9), anti-viral (10), anti-diabetes (11) and anticancer properties (12-14). During the past 10 years, numerous studies have reported that curcumin and its derivatives can effectively inhibit tumor cell growth, and induce apoptosis, autophagy and cell cycle arrest (4,12). Currently, numerous phase II and III clinical trials have advocated for the application of curcumin in patients with multiple myeloma, myelodysplastic syndromes, pancreatic cancer, head and neck cancer and colon cancer (15). In a previous clinical study, curcumin was proven to be safe even at doses of up to 8 g per day (16). Curcumin is, by all accounts, an ideal medication for the inhibition of cancer growth through various signaling pathways. However, certain animal and human pharmacokinetic studies have reported a poor absorption of curcumin in the gastrointestinal tract. The low systemic bioavailability of curcumin prevents an adequate concentration from reaching the target tissues to achieve pharmacological effects (17-20).

To overcome its poor bioavailability and increase its absorption *in vivo*, a novel curcumin derivative (1E,3Z,6E)-3-hydroxy-5-oxohepta-1,3,6-triene-1,7-diyl)bis(2-methoxy-4,1-phenylene) bis(3-hydroxy-2-hydroxymethyl)-2-methylpropanoate(MTH-3), was designed and developed. Fig. 1A includes a schematic of MTH-3. In a previous study it was demonstrated that, MTH-3 has superior hydrophilicity than curcumin. The log P, calculated logarithmic partition coefficient, of MTH-3 is 1.73, and of curcumin it is 3.38 (21,22). Furthermore, previous findings showed that MTH-3 inhibits tumor proliferation and induces apoptosis in TNBC *in vitro* and *in vivo* through cell cycle arrest and the autophagic pathway (21). Chang *et al* (22) revealed that MTH-3 has a greater inhibitory effect against TNBC cells compared with curcumin. That study also reported a 10-fold higher potency of MTH-3 compared to curcumin against doxorubicin-resistant MDA-MB-231 cell proliferation.

In the present study, the ability of MTH-3 to inhibit invasiveness in TNBC and the potential molecular signaling pathways were investigated.

Materials and methods

Chemicals. MTH-3 was synthesized and designed as previously described (21). Its chemical structure is shown in Fig. 1A. Hsieh *et al* (21) initially nominated the novel curcuminoid derivative as compound 9a, and the nomenclature was revised to MTH-3 in the study by Chang *et al* (22). L-glutamine, fetal bovine serum (FBS), streptomycin, Leibovitz's L-15 medium, penicillin G, and trypsin-EDTA were purchased from Thermo Fisher Scientific, Inc. Matrigel was obtained from Corning, Inc. Antibodies were purchased from Cell Signaling Technology, Inc. All other chemicals were purchased from Merck KGaA.

Cell culture. The MDA-MB-231 human breast adenocarcinoma cell line was obtained from the Bioresource Collection and Research Center (Hsinchu, Taiwan). MDA-MB-231 cells were cultured with 90% Leibovitz's L-15 medium, 1% penicillin-streptomycin and 10% FBS in 75 cm^2 culture flasks in an incubator with a humified 5% CO_2 atmosphere at 37˚C (23).

Cell viability assay. MTT assay was conducted to evaluate the cytotoxicity of MTH-3 in MDA-MB-231 cells. The initial concentration of tumor cells was $1x10^5$ cells/ml in a 96-well cell culture plate. Tumor cells were treated with various concentrations of MTH-3 (0, 1, 2, 3, 4 and 5 μM) at 37˚C. After 24 h of cell culture, MTT solution (0.5 mg/ml) was added, and the cells were incubated for an additional 4 h at 37˚C. Next, the formazan crystals were dissolved in DMSO following the removal of the medium. The formazan product was analyzed spectrophotometrically at a wavelength of 490 nm (24). This analysis was performed in triplicate.

TUNEL assay. MDA-MB-231 cells were cultured in 12-well plates and treated with different concentrations of MTH-3 (1, 2, 3, 4 and 5 μM) or with 0.1% DMSO in Leibovitz's L-15 medium at 37˚C for 24 h. Cells were collected and fixed with absolute ethanol. These cells were subsequently stained with DAPI solution to detect DNA breakdown using the *In Situ* Cell Death Detection Kit, Fluorescein (Roche Diagnostics GmbH) as previously described (25). This analysis was performed in triplicate.

Wound healing assay. For the wound healing assay, MDA-MB-231 cells were incubated untill they reached ~90% confluence in a tissue culture plate. Next, to creat a 1 mm wound area, each well of the culture plate was scratched using a micropipette tip. The tumor cells were subsequently cultured in serum-free Leibovitz's L-15 medium with MTH-3 at different concentrations (1, 2, 3 and 4 μM) or with 0.1% DMSO at 37˚C for 24 h. Tumor cells and the denuded zones were photographed under a phase-contrast microscope (magnification, x100) (26). This analysis was performed in triplicate.

Transwell assay. To investigate tumor cell invasion, a Transwell assay with a Matrigel®-coated invasion chamber was performed. Firstly, to form a genuine reconstituted basement membrane, the Transwell insert (polycarbonate filters with an 8-μm porosity) was coated with 30 μg Engelbreth-Holm-Swarm sarcoma tumor matrix (Matrigel®). Next, $1x10^6$ MDA-MB-231 cells were seeded in serum-free Leibovitz's L-15 medium in a T-75 culture plate. After 24 h of incubation, these tumor cells were suspended, and $5x10^4$ cells/chamber were subsequently added in the upper chamber of the Transwell insert with serum-free medium. The lower chamber contained Leibovitz's L-15 medium with 10% FBS. The tumor cells were treated with different concentrations of MTH-3 (1, 2, 3 and 4 μM) or with 0.1% DMSO at 37˚C for 24 h. After incubation for cancer cell invasion, the samples were fixed with 4% formaldehyde for

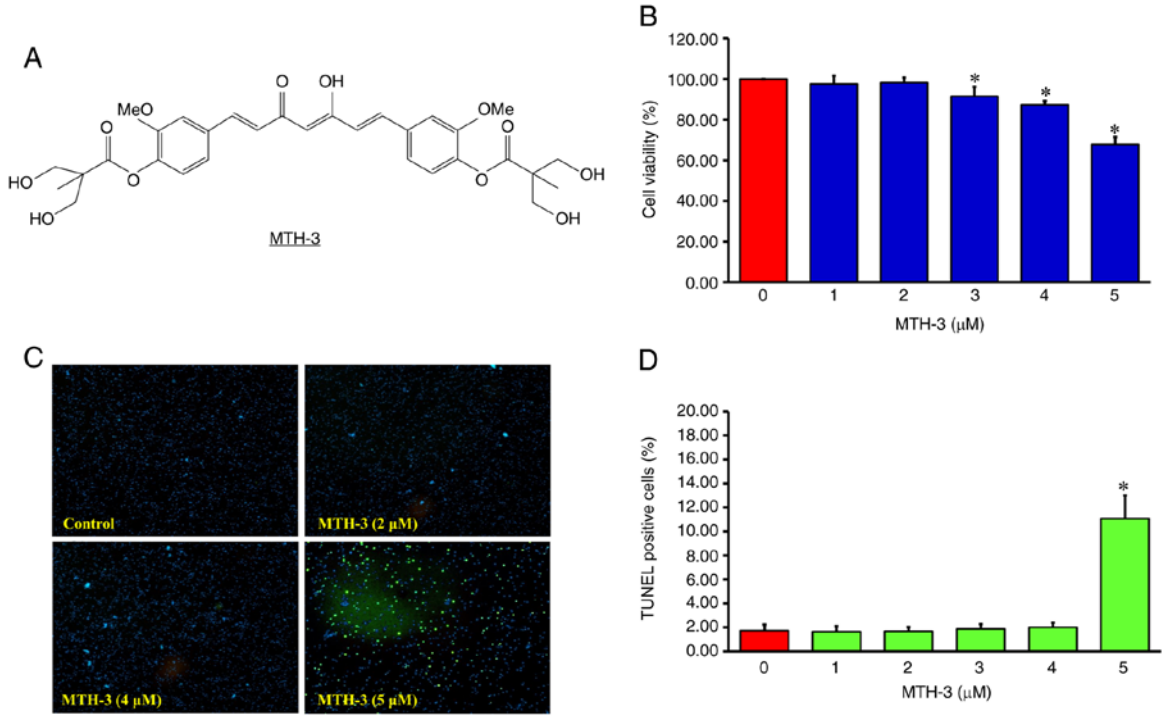

Figure 1. (A) Chemical structure of MTH-3. (B) Following treatment with 0, 1, 2, 3, 4 and 5 μM MTH-3 for 24 h, the cell viability of MDA-MB-231 cells was evaluated by MTT assay. (C and D) The proportions of apoptotic cell death was evaluated by TUNEL assay. Data are presented as the mean ± standard deviation of three experiments. *P<0.05. MTH-3, (1E,3Z,6E)-3-hydroxy-5-oxohepta-1,3,6-triene-1,7-diyl)bis(2-methoxy-4,1-phenylene)bis(3-hydroxy-2-hydroxymethyl)-2-methyl propanoate.

15 min. Next, 2% crystal violet was used for staining. Finally, the tumor cells in the upper chamber were removed, and the invading cells in the lower chamber were visualized under a light microscope (Leica Microsystems GmbH; magnification, x200) (26). This analysis was performed in triplicate.

Gelatin zymography. Gelatin zymography assay was performed to investigate the protein activity of matrix metalloproteinase (MMP)-2 and MMP-9. Firstly, MDA-MB-231 cells were treated with different concentrations of MTH-3 (1, 2, 3 and 4 μM) or with 0.1% DMSO in serum-free Leibovitz's L-15 medium at 37˚C for 24 h. These tumor cells were then suspended in zymography sample buffer. Next, the samples were added in loading buffer, and subsequently electrophoresed on 10% sodium dodecyl sulfate-polyacrylamide gel containing 0.1% gelatin. Subsequently, 2.5% Triton X-100 in double-distilled H_2O was used to wash the gels. The gels were then stored in development buffer (0.02% Briji-35, 1 mM $ZnCl_2$, 5 mM $CaCl_2$, 50 mM Tris, and 200 mM NaCl at pH 7.5) at 37˚C. After 18 h, the gels were stained with 0.5% Coomassie blue G-250. Then, the gels were de-stained. The non-staining bands indicated proteolytic activities. These results were analyzed using ImageJ software (National Institutes of Health) (27). This analysis was performed in triplicate.

3D spheroid invasion assay. Following the manufacturer's instructions, MDA-MB-231 cells ($5x10^3$ cells/total) were seeded into 96-well round-bottom ultralow attachment plates for 3 days. After the spheroid diameter reached 200-μm, MDA-MB-231 cells were treated with different concentrations of MTH-3 (1, 2, 3 and 4 μM) or with 0.1% DMSO. Matrigel solution was added, and the plate was placed in a 37˚C incubator for 30 min to polymerize the Matrigel. The system IncuCyte S3 ZOOM System instrument (Essen BioScience) was used to monitor spheroid invasion (28,29). This analysis was performed in triplicate.

Whole transcriptome sequencing (next-generation sequencing analysis). To evaluate the possible signaling pathways of MTH-3 in MDA-MB-231 cells, RNA sequencing analysis of MTH-3-exposed and control groups was performed. Total RNA extraction, quantification, as well as sequencing cluster generation and high throughput sequencing were performed using Illumina (New England Biolabs), according to the manufacturer's instructions. Every step was performed under strict monitoring and quality control. After mixing libraries based on the effective concentration and the required sequencing data volume, high throughput sequencing was conducted using a high throughput sequencing platform to capture and sequence the entire mRNA pool. Bioinformatics analysis was performed after obtaining the original sequence data, as previously described (30). These individual libraries were converted to the FASTQ format. The raw sequencing data eliminated the adapter sequences. Short-read alignment was performed using Hisat2 (v2.0.1) with the default parameters (31). Using the pipeline on the human reference genome from the UCSC Genome Browser, the paired-end reads were mapped. Differential mRNA expression analysis was conducted to identify over-represented functional terms presenting in the background. Benjamini-Hochberg false discovery rate correction and a Student's t-test were performed to determine significantly differentially expressed genes (DEGs). The

Kyoto Encyclopedia of Genes and Genomes (KEGG) database with the David/EASE tool was used for pathway analysis. Rich factor and q-value were applied to evaluate the degree of KEGG enrichment. The ratio of the number of DEGs to the number of total annotated genes in a certain pathway is shown by Rich factor, and Q value (0-1) is a multiple hypothesis-corrected P-value, which closer to 0 indicate a greater enrichment. Differentially expressed genes (DEGs) between MTH-3-exposed and control groups were selected using three criteria: P<0.005, adj P<0.05 and absolute fold change of ≥1.2). The DEGs were selected by multiple systemic analysis (30,32). This analysis was performed in duplicate.

Antibodies microarray analysis. To further evaluate the correlation between mRNA and protein expression levels, Kinex Antibody Microarray was used for subsequent analysis. Briefly, MDA-MB-231 cells were seeded in serum-free Leibovitz's L-15 medium at 37˚C with 2 μM MTH-3 or with 0.1% DMSO for 24 h. Tumor cells were then collected. From each sample, lysate proteins were labeled with proprietary fluorescent dye combination. After blocking the non-specific binding sites, the unbound proteins were washed away, and the chambers were displayed on the microarray. Images were captured using a Perkin-Elmer ScanArray Reader laser array scanner (Thermo Fisher Scientific, Inc.). ImaGene 9.0 (BioDiscovery) was used for spot segmentation and background correction. The overall average intensity of all spots within the samples was subtracted from the raw intensity of each spot to calculate the Z scores (33). Z ratios were calculated by dividing the difference between the averages of the observed protein Z scores by the standard deviations of all the differences for a particular comparison. Z ratio values of ±1.2 were considered statistically significant (33). This analysis was performed in triplicate.

Western blot analysis. To further analyze the protein expression levels, western blot analysis was performed. Briefly, MDA-MB-231 cells were cultured in Leibovitz's L-15 medium at 37˚C with 2 μM MTH-3 or with 0.1% DMSO for 24 h. Tumor cells were then collected to obtain the protein lysate. Bio-Rad protein assay system (Bio-Rad Laboratories, Inc.) was used for determination of protein concentrations. These samples (35 μg per lane) were separated via 10-12% SDS-PAGE and transferred to PVDF membranes. The membranes were blocked with 5% skimmed dry milk at room temperature for 2 h. The membranes were incubated overnight at 4˚C with primary antibodies purchased from Cell Signaling Technology, Inc., including AKT (cat. no. GTX121937; dilution, 1:5,000), p-AKT (phospho Ser473, cat. no. GTX28932; dilution, 1:400), ERK (cat. no. GTX59618; dilution, 1:10,000), p-ERK (phospho Thr202/Tyr204, cat. no. GTX59568; dilution, 1:10,000), p38/MAPK (cat. no. GTX110720; dilution, 1:1,000), p-p38/MAPK (cat. no. GTX48614; dilution, 1:500), JNK (cat. no. GTX52360; dilution, 1:500), p-JNK (phospho Thr183/Tyr185, cat. no. GTX52326; dilution, 1:500), and β-actin (cat. no. GTX109639; dilution, 1:10,000). Subsequently, the membranes were incubated for 4 h at room temperature with horseradish peroxidase-conjugated secondary antibodies, including anti-rabbit IgG (cat. no. 7074; dilution, 1:10,000) and anti-mouse IgG (cat. no. 7076; dilution, 1:10,000). Finally, the protein bands were visualized using ECL reagents (Cytiva) and scanned on a UMAX powerLook Scanner (UMAX Technologies). The National Institutes of Health ImageJ 1.52v program was used for quantitative analysis of the intensity of the band signal. This analysis was performed in quadruplicate.

Statistical analysis. Data are presented as the mean ± standard deviation. One-way analysis of variance followed by Dunnett's test and Tukey's post hoc test was conducted to analyze the differences between two groups and among multiple groups, respectively, using SPSS software version 25.0 (IBM, Corp.). P<0.05 was considered to indicate a statistically significant difference (34).

Results

MTH-3 inhibits the proliferation in MDA-MB-231 human breast adenocarcinoma cells. The tumor cells were treated with different concentrations of MTH-3 (1, 2, 3, 4 and 5 μM) or with 0.1% DMSO at 37˚C for 24 h. The cells were suspended and analyzed by MTT method to detect the cell viability. The results showed a significantly reduced viability after 3, 4 and 5 μM MTH-3 at 91.45±4.69, 89.27±3.34 and 67.83±3.62%, respectively (Fig. 1B).

On the other hand, as shown in Fig. 1C and D, MTH-3 treatment at a concentration of 1-4 μM did not significantly induce apoptotic cell death, revealed by TUNEL assay. As a result, the concentrations of 1, 2, 3 and 4 μM of MTH-3 were subsequently selected to further study the effects on MDA-MB-231 cell invasion and metastasis.

MTH-3 inhibits invasion and migration in MDA-MB-231 human breast adenocarcinoma cells. The tumor cells were incubated with various concentrations of MTH-3 (1, 2, 3 and 4 μM) or with 0.1% DMSO at 37˚C for 24 h to determine their ability of cell migration and invasion abilities by Transwell, wound healing and 3D spheroid invasion assays. In Fig. 2A and B, the tumor cells were found to be significantly decreased in the lower chamber in the MTH-3 treatment groups. In Fig. 2C and D, the edge distance in MTH-3 treatment groups was significantly wider than that in the control group, indicating that MTH-3 inhibited MDA-MB-231 cell motility in a concentration-dependent manner. To develop a tumor cell invasion and migration model, 3D spheroid invasion assay was applied to recapitulate both biochemical and physical characteristics of the tumor microenvironment. In Fig. 3A and B, MTH-3 significantly inhibited tumor spheroid invasion and migration in the Matrigel-coated area. These results suggested that MTH-3 inhibited MDA-MB-231 cells invasion and migration in a concentration-dependent manner. In combination, these data suggested that a concentration of <5 μM MTH-3 predominantly inhibited tumor cell migration and invasion. However, MTH-3-exhibited toxicity in MDA-MB-231 cells may require higher concentrations or longer incubation times.

MTH-3 suppresses the activity of MMP-9 in MDA-MB-231 human breast adenocarcinoma cells. Gelatin zymography was performed to further determine the role of MMP-2/-9 activity in MTH-3-treated MDA-MB-231 cells. Following MTH-3 treatment for 24 h, the conditioned media of tumor cells with different concentrations of MTH-3 (1, 2, 3 and 4 μM) or with

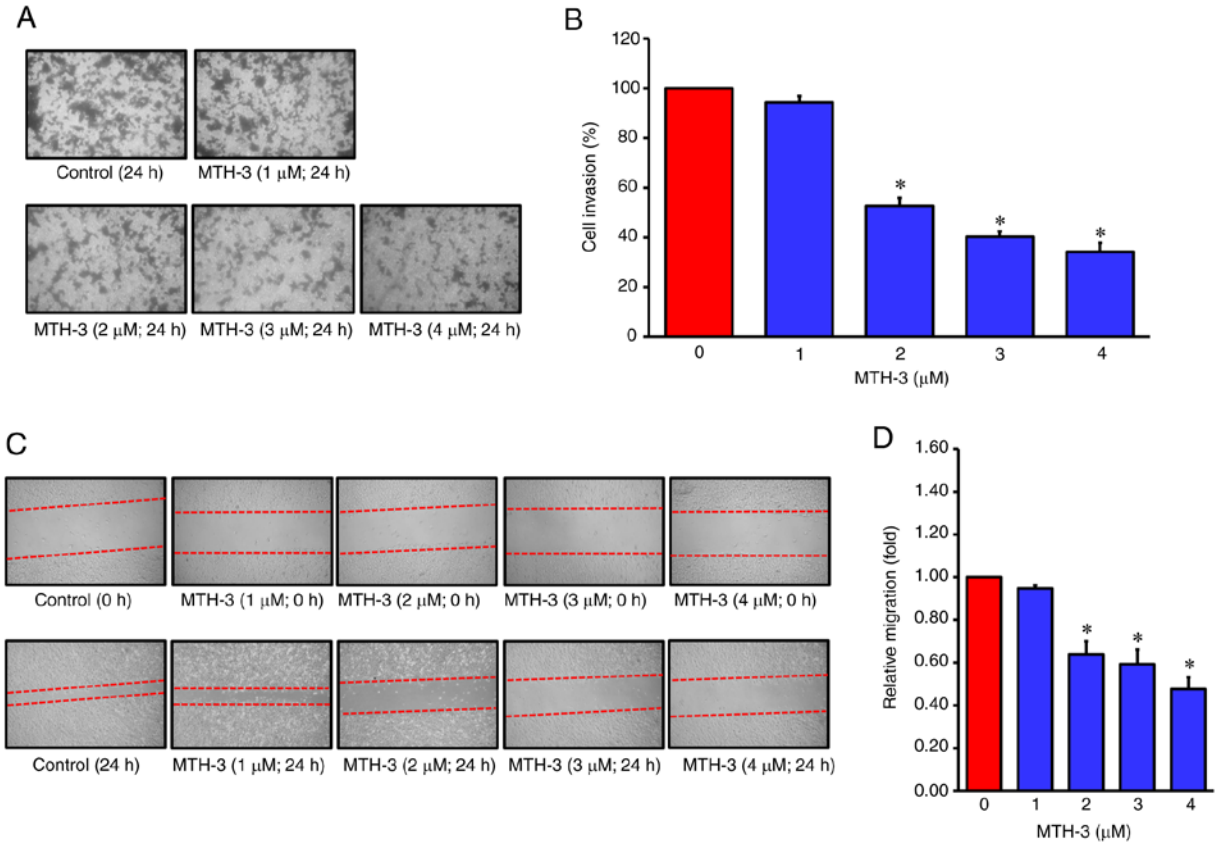

Figure 2. MTH-3 suppressed invasion and migration in human breast adenocarcinoma MDA-MB-231 cells. (A) The invasion ability of MDA-MB-231 cells was evaluated using a Matrigel®-coated invasion chamber. Following treatment with various concentrations of MTH-3 for 24 h, the invading MDA-MB-231 cells in the lower chamber were stained and subsequently counted under a light microscope (magnification, x200). (B) Tumor cell invasion was semi-quantified. (C) The ability of migration of MDA-MB-231 cells was evaluated by wound healing assay. Following treatment with the various concentrations of MTH-3 for 24 h in serum-free Leibovitz's L-15 medium, MDA-MB-231 cells were photographed. (D) The migrated tumor cells were quantified. Data are presented as the mean ± standard deviation of three experiments. *P<0.05. MTH-3, (1E,3Z,6E)-3-hydroxy-5-oxohepta-1,3,6-triene-1,7-diyl)bis(2-methoxy-4,1-phenylene) bis(3-hydroxy-2-hydroxymethyl)-2-methyl propanoate.

0.1% DMSO were collected to measure the gelatinase activity of MMP-2 and -9. The results revealed that MTH-3 decreased MMP-9 activity in a concentration-dependent manner in MDA-MB-231 cells *in vitro* (Fig. 3C and D).

MTH-3 inhibits invasion through the MAPK/ERK/AKT signaling pathway and causes cell cycle arrest in MDA-MB-231 human breast adenocarcinoma cells. To gain insight into the biological activity of MTH-3 in MDA-MB-231 cells, RNA sequencing transcriptional profile analysis was performed. As shown in Fig. 4A, three replicates for normalized RNA-sequencing data from MTH-3-treated samples and the control group were clustered separately using unsupervised Principal Component Analysis, indicating a significantly different Gene Expression Omnibus analysis. Genes in blue were highly expressed, and those in red were expressed at low levels. Fig. 4B shows the differential expression of an MA plot. Red dots represent significantly upregulated genes, and blue dots symbolized significantly downregulated genes. Fig. 4C contains a bar graph of significantly up- or downregulated genes between MTH-3-treated and control groups. A total of 315 genes were upregulated and 648 downregulated. To further determine the physiological activities of the genes and associated functions, the KEGG database were used (35). KEGG pathway analysis and hypergeometric tests were performed to identify the pathways of the DEGs and related pathways that were significantly enriched compared to the transcriptome background. In Fig. 4D, the scatter plot is used for the graphical representation of the KEGG pathway enrichment analysis, which is measured by the Rich factor, Q-value, and the number of genes enriched in these pathways. The top 20 KEGG pathways, most significantly enriched for the analysis, were selected and shown. The enriched KEGG pathways are shown in Fig. 5. Genes in red are upregulated and those in blue are downregulated. Gene ontology (GO) enrichment analysis revealed that the MTH-3-altered expression of genes was largely associated with the MAPK/ERK/AKT signaling cascade and cell cycle pathway. The sequencing raw data are shown in Table SI.

Subsequently, the protein expression levels were examined using antibody microarray analysis and western blot analysis to investigate the correlation between mRNA and protein expression levels, since mRNA expression analysis can be inaccurate and potentially misleading (33). The results presented in Table I revealed that MTH-3 treatment significantly downregulated phosphorylated MAPK p38α, MAPK/ERK protein-serine kinase (MEK2), ERK1/2 and proline-rich AKT substrate 40 kDa (PRAS40). Furthermore, MTH-3 significantly downregulated phosphorylated Cyclin A, Cyclin D1, cell division control protein 42 (CDC42) and cyclin-dependent protein-serine kinase 2 (CDK2). As shown in Fig. 6, the protein

Table I. Summary of antibody microarray analyses[a].

Antibody codes	Target protein name	Phospho site (Human)	% CFC (MTH-3 from CTL)	Z-ratio (MTH-3, CTL)
NN024	CDC42	Pan-specific	-44	-1.76
NK026-3	CDK2	Pan-specific	-34	-1.26
NN028	Cyclin A	Pan-specific	-51	-2.03
NN030-1	Cyclin D1	Pan-specific	-71	-3.49
PK170-PK171	ERK1/2	T202+T185	-35	-1.31
NK120-2	p38/MAPK	Pan-specific	-36	-1.31
NK120-4	p38a/MAPK	Pan-specific	-43	-1.68
PK049-2	MEK2	T394	-52	-2.18
PN062	Proline-rich Akt substrate 40 kDa (PRAS40)	T246	-47	-1.88

[a]Significant downregulation of phosphorylated ERK1/2, MAPK p38, MEK2, PRAS40, cyclin A, cyclin D1, CDC42 and CDK2. % CFC indicates the percentage change in the normalized intensity of the MTH-3-treated sample compared with the control. A Z ratio of ±1.2 was considered significant. MEK2, MAPK/ERK protein-serine kinase; PRAS40, proline-rich AKT substrate 40 kDa; CDC42, cell division control protein 42; CDK2, cyclin-dependent protein-serine kinase 2; CTL, control.

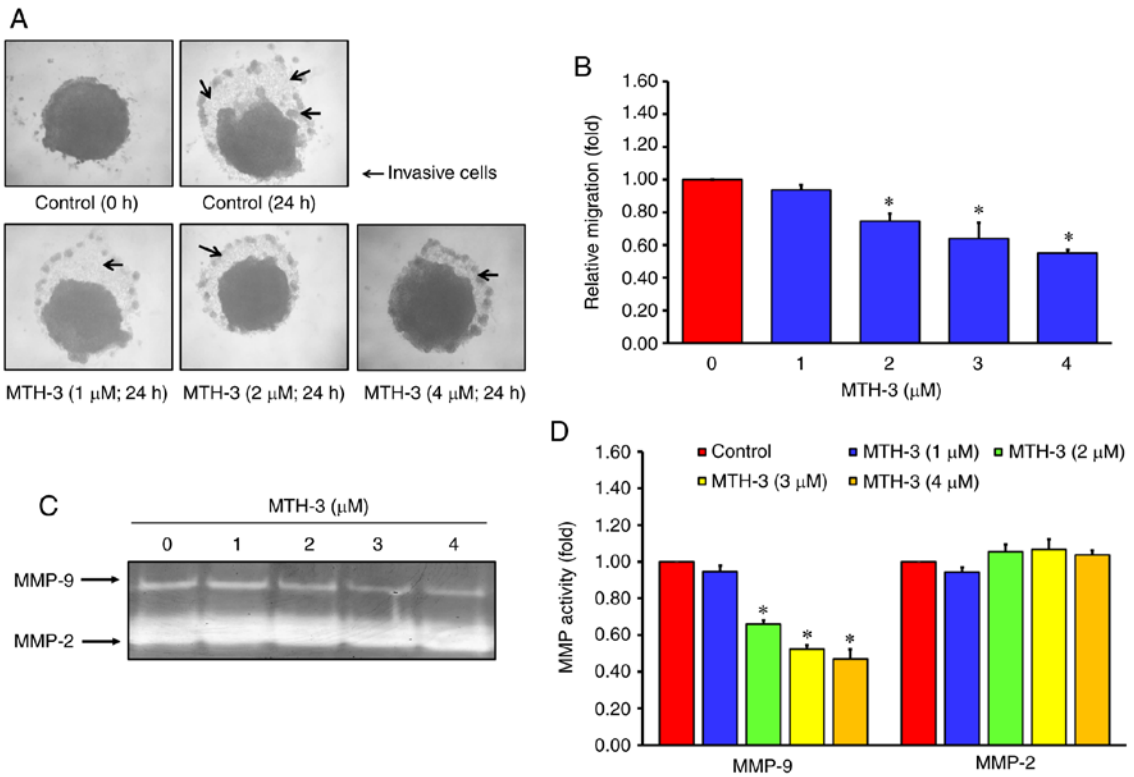

Figure 3. MTH-3 inhibited MMP-9 activity, and suppressed tumor spheroid invasion and migration in MDA-MB-231 human breast adenocarcinoma cells. (A) To mimic the complexity and heterogeneity of clinical tumors, a 3D spheroid invasion assay was performed. Following treatment with the indicated concentrations of MTH-3 for 24 h, MTH-3 significantly inhibited MDA-MB-231 spheroid invasion in the Matrigel-coated area, and (B) cell invasion was semi-quantified. Arrows indicate invasive tumor cells. (C) The activity of MMP-2 and -9 was evaluated by gelatin zymography, and (D) the results were quantified. Data are presented as the mean ± standard deviation of three experiments. *P<0.05. MTH-3, (1E,3Z,6E)-3-hydroxy-5-oxohepta-1,3,6-triene-1,7-diyl) bis(2-methoxy-4,1-phenylene)bis(3-hydroxy-2-hydroxymethyl)-2-methyl propanoate.

expression of p-AKT, p-ERK, p-p38 and p-JNK was decreased. In combination, the present results demonstrated that MTH-3 suppressed the MAPK/ERK/AKT signaling pathway and cell cycle-related protein phosphorylation in MDA-MB-231 human breast adenocarcinoma cells. The original images of the integral western blot gels are shown in Fig. S1.

Discussion

MTH-3 is a novel bis(hydroxymethyl) alkanoate curcuminoid derivative, designed by Hsieh *et al* (21). Findings of that study revealed that MTH-3 was effective against numerous breast cancer cell lines and induced limited toxicity to normal

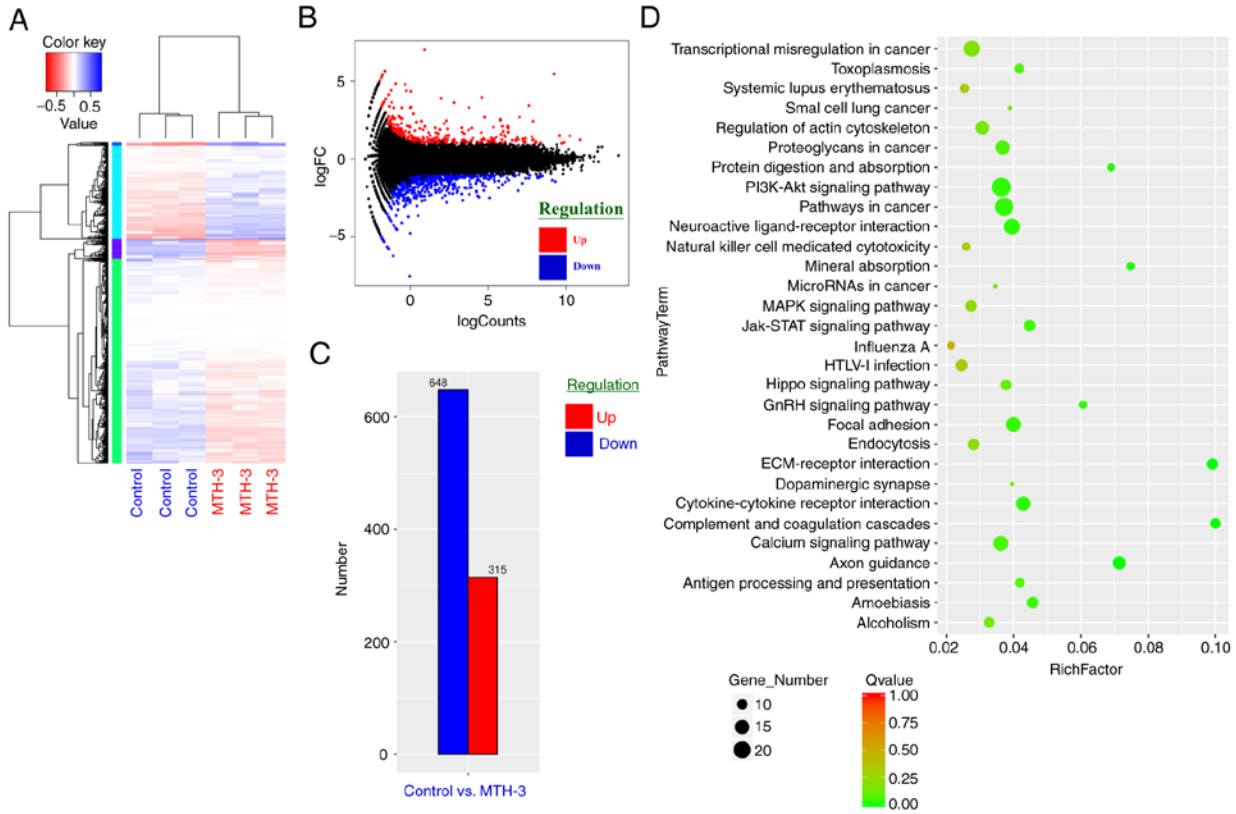

Figure 4. RNA-sequencing transcriptional profile analysis was performed to gain insight into the biologic activity induced by MTH-3 in MDA-MB-231 cells. (A) The log10 (RPKM + 1) values of differentially expressed genes were used for cluster analysis. Genes with a high expression are shown in blue and those with a low expression in red. (B) Differential expression of MA plot. Red dots represent significantly upregulated genes and blue dots significantly downregulated genes. (C) Bar graph of genes that were significantly up- or downregulated between the MTH-3-treated and control groups. (D) Scatter plot representing the KEGG enrichment of differentially expressed genes. x-axis, rich Factor; y-axis, KEGG pathways. The number of differentially expressed genes in the pathway is positively correlated to the size of these dots. Color coding indicates different value ranges. KEGG, Kyoto Encyclopedia of Genes and Genomes. MTH-3, (1E,3Z,6E)-3-hydroxy-5-oxohepta-1,3,6-triene-1,7-diyl)bis(2-methoxy-4,1-phenylene)bis(3-hydroxy-2-hydroxymethyl)-2-methyl propanoate.

tissues in an established xenograft nude mouse model of MDA-MB-231 cells. In addition, Chang *et al* (22) identified a synergistic activity of MTH-3 combined with doxorubicin in the inhibition of MDA-MB-231 cell growth. MTH-3 treatment induced cell cycle arrest, as well as the apoptotic and autophagic pathways in MDA-MB-231 cells. To the best of our knowledge, the present study was the first to demonstrate that MTH-3 inhibited the invasion of MDA-MB-231 cells and elucidate the potential signaling pathways. In anti-metastasis drug discovery, the compounds not only exhibit the cytotoxic effect at high concentrations but also possess anti-metastasis activity at low concentrations (36). Our previous findings demonstrated that MTH-3 inhibited cell proliferation and induced G_2/M arrest, cell autophagy and apoptosis at a high concentration (>5 μM) in MDA-MB-231 cells. Results of the present study revealed that a low concentration (2, 3 and 4 μM) of MTH-3 predominantly inhibited MDA-MB-231 tumor cell migration and invasion (Figs. 2 and 3), but did not induce cell apoptosis by TUNEL assay (Fig. 1C and D).

Curcumin has been proven to be safe and effective in inhibiting cancer cell growth (16). However, poor gastric absorption and low systemic bioavailability prevent the pharmacological properties of curcumin from reaching the target tissues. Researchers have developed several methods to overcome the poor hydrophilicity of curcumin, including nanoparticles, liposomes, phospholipid complexes, micelles, and cyclodextrin encapsulation (37). Furthermore, the half-life of curcumin is short, resulting in low bioavailability. Several novel derivatives of curcumin have been developed to delay the metabolism into glucuronides and sulfates through a phase II transformation, replacing its phenolic OH groups with ester (38,39). MTH-3, a novel curcumin derivative designed by Hsieh *et al* (21), was proven to have a superior solubility in water and alcohol than curcumin in the previous study, with a 10-fold higher potency.

MTH-3 significantly inhibited MDA-MB-231 cell invasion and migration in the present study. Cancer metastasis is a complex process. The basement membrane and extracellular matrix are major physical barriers to inhibiting cancer cell invasion and migration (26). MMPs play a key role in degrading the basement membrane and extracellular matrix. Previous findings have shown that tumor cells can specifically produce MMP-2 and -9 to destroy these natural barriers, resulting in the invasion and migration of tumor cells into adjacent tissue and blood vessels (40). MMP-2, which can degrade type V, VI and X collagens, gelatins and IV collagen in the basement membrane, was found to be constitutively expressed in various tissues, including cancer cells, rather than as part of the initial response to invasion (41). MMP-9 can be secreted extracellularly to degrade type IV collagens and fibronectins, which can be stimulated by various inflammatory cytokines and growth factors during pathological processes, including affecting

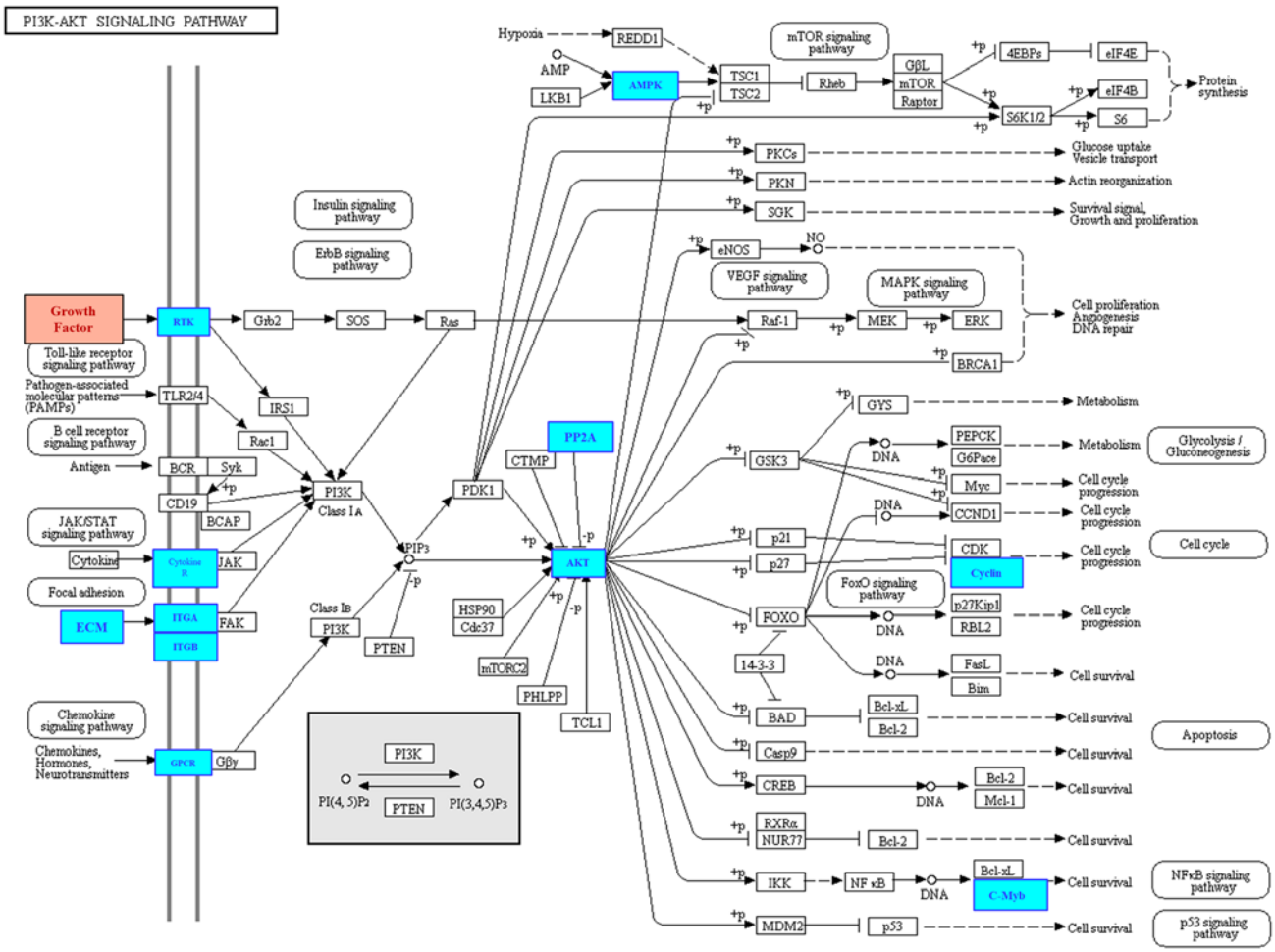

Figure 5. Significant suppression of the KEGG MAPK/ERK/AKT signaling pathway and cell cycle cascade. KEGG, Kyoto Encyclopedia of Genes and Genomes.

the adhesion ability of tumor cells (42). The results of the present study showed that MTH-3 inhibits MDA-MB-231 cell invasion and migration by decreasing the activity of MMP-9, instead of that of MMP-2. These results were consistent with those reported by Fan *et al* (43), who demonstrated that casticin inhibits MMP-9 protein expression and activity in breast cancer cells.

Numerous studies have demonstrated the anti-metastasis effects of curcumin in breast cancer cells. Coker-Gurkan *et al* reported that curcumin inhibits invasion and metastasis by targeting NF-κB signaling in breast cancer cell lines, including MCF-7, MDA-MB-453 and MDA-MB-231 (45). Gallardo and Calaf (46) and Hu *et al* (47) reported curcumin induces anti-metastasis activity through epithelial-mesenchymal transition. Guan *et al* (48) reported that curcumin suppresses migration in MDA-MB-231 cells through PI3K/AKT signaling pathway. To the best of our knowledge, the present study was the first to report that MTH-3, a novel curcuminoid derivative, suppresses tumor invasion in breast cancer. The possible signal transduction was further investigated.

Next-generation sequencing (NGS)-based molecular diagnosis and analysis is becoming one of the major tools of personalized treatment and drug development (49). RNA expression profile analysis provides a more accurate analysis of the tumor phenotype compared with genome analysis, which makes it the most powerful tool of high throughput quantitative transcriptomics (50). The expression levels of targets of molecular medicines were analyzed and profiling of the activation of the relevant molecular pathways was used to enable the personalized prescription of a wide range of molecular-targeted therapies (51). To evaluate the possible signaling pathways of MTH-3 in MDA-MB-231 cells, whole transcriptome sequencing analysis of MTH-3-exposed and control groups was performed in the present study. The results showed that MTH-3-altered gene expressions were markedly associated with cell invasion and MAPK/ERK/AKT signaling pathway. The MAPK/ERK/AKT signaling pathway was suppressed in MDA-MB-231 human breast adenocarcinoma cells after MTH-3 treatment, as shown in Fig. 5. Inhibition of the signaling transduction was confirmed by western blot analysis, as shown in Fig. 6. Furthermore, cell cycle-related gene expression was also decreased. Since mRNA expression analysis can be inaccurate and potentially misleading, antibody microarray analysis was subsequently performed to investigate the correlation between mRNA and protein expression levels (52,53). The results in Table I revealed that treatment of MTH-3 significantly downregulated phosphorylated ERK1/2, p38/MAPK, MEK2 and proline-rich Akt substrate 40 kDa (PRAS40). MTH-3 also significantly downregulated phosphorylated cyclins A and D1, CDC42 and CDK2.

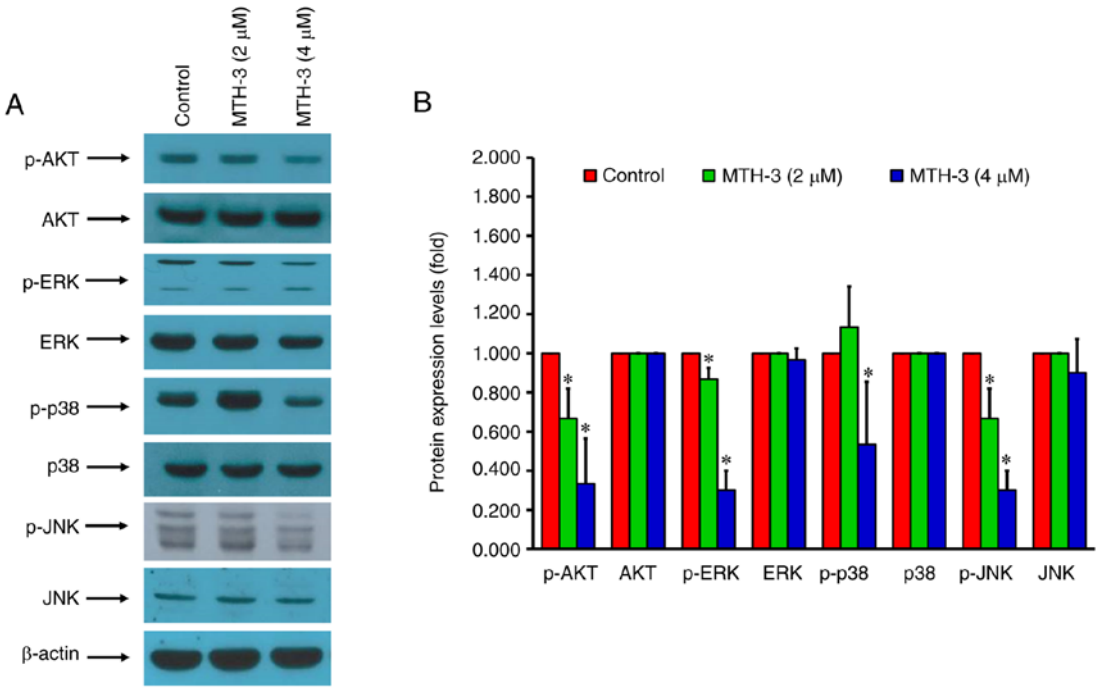

Figure 6. MTH-3 modulates MAPK/ERK/AKT signaling-related protein levels in MDA-MB-231 human breast adenocarcinoma cells. (A) Western blot analysis shows a decreased expression of p-AKT, p-ERK, p-p38/MAPK and p-JNK proteins. (B) Quantitative analysis of the intensities of protein bands. MTH-3, (1E,3Z,6E)-3-hydroxy-5-oxohepta-1,3,6-triene-1,7-diyl)bis(2-methoxy-4,1-phenylene)bis(3-hydroxy-2-hydroxymethyl)-2-methyl propanoate; p-, phosphorylated.

The MAPK/ERK and PI3K/AKT signaling pathways play an important role in cancer cell survival, proliferation, apoptosis, invasion and metastasis (54,55). The aberrant activation of this signaling pathway induces the survival, proliferation and metastasis of breast cancer cells (54). Chen e*t al* (56) reported that curcumin inhibits doxorubicin-induced epithelial-mesenchymal transition through the suppression of PI3K/AKT and TGF-β signaling transduction in TNBC. Berrak *et al* (57) reported that curcumin induced cell cycle arrest and inhibited PI3K signaling transduction in MCF-7 breast cancer cells. Guan *et al* (48) demonstrated that curcumin suppresses proliferation and migration through autophagy-dependent AKT degradation in MDA-MB-231 cells.

Furthermore, several studies have demonstrated that cyclin proteins regulate tumor cell invasion and metastasis. Cell cycle arrest inhibits tumor invasion and metastasis (58-61). Fusté *et al* (58), Body *et al* (62), and Chen *et al* (63) reported that cyclin D1 fosters tumor cell invasion and metastasis through cytoplasmic mechanisms. CDC42 knockdown was shown to inhibit tumor cell migration and invasion, and be associated with the downregulation of cyclins A, D1 and E/CDK2 (14,59,60,64). In previous studies, MTH-3 was found to inhibit TNBC cell proliferation and induce apoptosis through the autophagic pathway and cause cell cycle arrest with a higher potency than curcumin (21,22). The present study demonstrated the ability of MTH-3 to inhibit the invasion of TNBC cells through the MAPK/ERK/AKT signaling pathways and cell cycle regulatory cascade.

In conclusion, the present study revealed that MTH-3 inhibits tumor invasiveness via the MAPK/ERK/AKT signaling pathway and cell cycle regulatory cascade in human adenocarcinoma MDA-MB-231 cells. Significant information with respect to the possible signal transduction of MTH-3 in TNBC was provided in the current study, and the results suggested that MTH-3 may be used in the treatment of breast cancer medication in the future.

Acknowledgements

This study was supported in part through the Medical Research Core Facilities, Office of Research and Development at China Medical University (Taichung, Taiwan), and Yen Tjing Ling Medical Foundation (Taipei, Taiwan). We also thank Mr. Kai-Hsiang Chang and Mr. Chin-Chen Lin (Tekon Scientific Corp.) and Mr. Chang-Wei Li (AllBio Science Incorporated, Taiwan) for their assistance and support with the equipment in this study.

Funding

Funding for this study was provided in part by China Medical University Hospital, Taichung, Taiwan (DMR-109-147), Ministry of Science and Technology, Taiwan (MOST 109-2320-B-039-041-), Taipei Veterans General hospital, Taipei, Taiwan (V110B-038), and Yen Tjing Ling Medical Foundation, Taipei, Taiwan (CI-110-6). Chinese Medicine Research Center, China Medical University from The Featured Areas Research Center Program within the framework of the Higher Education Sprout Project by the Ministry of Education (MOE) in Taiwan also provided partial support.

Availability of data and materials

Data of transcriptome sequencing in this published article have been uploaded to the European Nucleotide Archive. Accession no.: ERP128028.

Authors' contributions

YJC, FJT, SCK and JSY contributed to the study design. YJC, DTB, LCC, MTH and JSY conducted the experiments. YJC, FJT, CCL and JSY analyzed the data. YJC, CCL and JSY confirmed the authenticity of all the raw data. YJC, CCL, JSY, and SCK wrote and revised the paper. All authors read and approved the final manuscript.

Ethics approval and consent to participate

Not applicable.

Patient consent for publication

Not applicable.

Competing interests

The authors declare that they have no competing interests.

References

1. McGuire A, Brown JA, Malone C, McLaughlin R and Kerin MJ: Effects of age on the detection and management of breast cancer. Cancers (Basel) 7: 908-929, 2015.
2. Feng Y, Spezia M, Huang S, Yuan C, Zeng Z, Zhang L, Ji X, Liu W, Huang B, Luo W, *et al*: Breast cancer development and progression: Risk factors, cancer stem cells, signaling pathways, genomics, and molecular pathogenesis. Genes Dis 5: 77-106, 2018.
3. Key TJ, Bradbury KE, Perez-Cornago A, Sinha R, Tsilidis KK and Tsugane S: Diet, nutrition, and cancer risk: What do we know and what is the way forward? BMJ 368: m511, 2020.
4. Wang X, Zhang H and Chen X: Drug resistance and combating drug resistance in cancer. Cancer Drug Resist 2: 141-160, 2019.
5. Chen T, Xiong H, Yang JF, Zhu XL, Qu RY and Yang GF: Diaryl ether: A privileged scaffold for drug and agrochemical discovery. J Agric Food Chem 68: 9839-9877, 2020.
6. Newman DJ and Cragg GM: Natural products as sources of new drugs over the 30 years from 1981 to 2010. J Nat Prod 75: 311-335, 2012.
7. Niwa T, Yokoyama Si, Mochizuki M and Osawa T: Curcumin metabolism by human intestinal bacteria in vitro. J Func Foods 61: 103463, 2019.
8. Yang H, Du Z, Wang W, Song M, Sanidad K, Sukamtoh E, Zheng J, Tian L, Xiao H, Liu Z and Zhang G: Structure-activity relationship of curcumin: Role of the methoxy group in anti-inflammatory and anticolitis effects of curcumin. J Agric Food Chem 65: 4509-4515, 2017.
9. Jing S, Zou H, Wu Z, Ren L, Zhang T, Zhang J and Wei Z: Cucurbitacins: Bioactivities and synergistic effect with small-molecule drugs. J Func Foods 72: 104042, 2020.
10. Mathew D and Hsu WL: Antiviral potential of curcumin. J func foods 40: 692-699, 2018.
11. Zaheri Z, Fahremand F, Rezvani ME, Karimollah A and Moradi A: Curcumin exerts beneficial role on insulin resistance through modulation of SOCS3 and Rac-1 pathways in type 2 diabetic rats. J Func Foods 60: 103430, 2019.
12. Tomeh MA, Hadianamrei R and Zhao X: A review of curcumin and its derivatives as anticancer agents. Int J Mol Sci 20: 1033, 2019.
13. Bondì ML, Emma MR, Botto C, Augello G, Azzolina A, Di Gaudio F, Craparo EF, Cavallaro G, Bachvarov D and Cervello M: Biocompatible lipid nanoparticles as carriers to improve curcumin efficacy in ovarian cancer treatment. J Agric Food Chem 65: 1342-1352, 2017.
14. DiMarco-Crook C, Rakariyatham K, Li Z, Du Z, Zheng J, Wu X and Xiao H: Synergistic anticancer effects of curcumin and 3',4'-didemethylnobiletin in combination on colon cancer cells. J Food Sci 85: 1292-1301, 2020.
15. Shehzad A, Wahid F and Lee YS: Curcumin in cancer chemoprevention: Molecular targets, pharmacokinetics, bioavailability, and clinical trials. Arch Pharm (Weinheim) 343: 489-499, 2010.
16. Shanmugam MK, Rane G, Kanchi MM, Arfuso F, Chinnathambi A, Zayed ME, Alharbi SA, Tan BK, Kumar AP and Sethi G: The multifaceted role of curcumin in cancer prevention and treatment. Molecules 20: 2728-2769, 2015.
17. Yang KY, Lin LC, Tseng TY, Wang SC and Tsai TH: Oral bioavailability of curcumin in rat and the herbal analysis from *Curcuma longa* by LC-MS/MS. J Chromatogr B Analyt Technol Biomed Life Sci 853: 183-189, 2007.
18. Marczylo TH, Verschoyle RD, Cooke DN, Morazzoni P, Steward WP and Gescher AJ: Comparison of systemic availability of curcumin with that of curcumin formulated with phosphatidylcholine. Cancer Chemother Pharmacol 60: 171-177, 2007.
19. Ma Y, Chen S, Liao W, Zhang L, Liu J and Gao Y: Formation, physicochemical stability, and redispersibility of curcumin-loaded rhamnolipid nanoparticles using the pH-Driven method. J Agric Food Chem 68: 7103-7111, 2020.
20. Cuomo F, Perugini L, Marconi E, Messia MC and Lopez F: Enhanced curcumin bioavailability through nonionic surfactant/caseinate mixed nanoemulsions. J Food Sci 84: 2584-2591, 2019.
21. Hsieh MT, Chang LC, Hung HY, Lin HY, Shih MH, Tsai CH, Kuo SC and Lee KH: New bis (hydroxymethyl) alkanoate curcuminoid derivatives exhibit activity against triple-negative breast cancer in vitro and in vivo. Eur J Med Chem 131: 141-151, 2017.
22. Chang LC, Hsieh MT, Yang JS, Lu CC, Tsai FJ, Tsao JW, Chiu YJ, Kuo SC and Lee KH: Effect of bis (hydroxymethyl) alkanoate curcuminoid derivative MTH-3 on cell cycle arrest, apoptotic and autophagic pathway in triple-negative breast adenocarcinoma MDA-MB-231 cells: An *in vitro* study. Int J Oncol 52: 67-76, 2018.
23. Wu KM, Hsu YM, Ying MC, Tsai FJ, Tsai CH, Chung JG, Yang JS, Tang CH, Cheng LY, Su PH, *et al*: High-density lipoprotein ameliorates palmitic acid-induced lipotoxicity and oxidative dysfunction in H9c2 cardiomyoblast cells via ROS suppression. Nutr Metab (Lond) 16: 36, 2019.
24. Lin KH, Li CY, Hsu YM, Tsai CH, Tsai FJ, Tang CH, Yang JS, Wang ZH and Yin MC: Oridonin, A natural diterpenoid, protected NGF-differentiated PC12 cells against MPP^+-and kainic acid-induced injury. Food Chem Toxicol 133: 110765, 2019.
25. Ha HA, Chiang JH, Tsai FJ, Bau DT, Juan YN, Lo YH, Hour MJ and Yang JS: Novel quinazolinone MJ-33 induces AKT/mTOR-mediated autophagy-associated apoptosis in 5FU-resistant colorectal cancer cells. Oncol Rep 45: 680-692, 2021.
26. Chiu YJ, Hour MJ, Jin YA, Lu CC, Tsai FJ, Chen TL, Ma H, Juan YN and Yang JS: Disruption of IGF-1R signaling by a novel quinazoline derivative, HMJ-30, inhibits invasiveness and reverses epithelial-mesenchymal transition in osteosarcoma U-2 OS cells. Int J Oncol 52: 1465-1478, 2018.
27. Liu SC, Tsai CH, Wu TY, Tsai CH, Tsai FJ, Chung JG, Huang CY, Yang JS, Hsu YM, Yin MC, *et al*: Soya-cerebroside reduces IL-1β-induced MMP-1 production in chondrocytes and inhibits cartilage degradation: Implications for the treatment of osteoarthritis. Food Agric Immunol 30: 620-632, 2019.
28. Vinci M, Box C and Eccles SA: Three-dimensional (3D) tumor spheroid invasion assay. J Vis Exp: e52686, 2015.
29. Howes AL, Richardson RD, Finlay D and Vuori K: 3-Dimensional culture systems for anti-cancer compound profiling and high-throughput screening reveal increases in EGFR inhibitor-mediated cytotoxicity compared to monolayer culture systems. PLoS One 9: e108283, 2014.
30. Stacchiotti S, Pantaleo MA, Negri T, Astolfi A, Tazzari M, Dagrada GP, Urbini M, Indio V, Maestro R, Gronchi A, *et al*: Efficacy and biological activity of imatinib in metastatic dermatofibrosarcoma protuberans (DFSP). Clin Cancer Res 22: 837-846, 2016.
31. Kim D, Langmead B and Salzberg SL: HISAT: A fast spliced aligner with low memory requirements. Nat Methods 12: 357-360, 2015.
32. Kanehisa M: Toward understanding the origin and evolution of cellular organisms. Protein Sci 28: 1947-1951, 2019.
33. Cheadle C, Vawter MP, Freed WJ and Becker KG: Analysis of microarray data using Z score transformation. J Mol Diagn 5: 73-81, 2003.
34. Chiu YJ, Yang JS, Hsu HS, Tsai CH and Ma H: Adipose-derived stem cell conditioned medium attenuates cisplatin-triggered apoptosis in tongue squamous cell carcinoma. Oncol Rep 39: 651-658, 2018.
35. Plaimas K, Mallm JP, Oswald M, Svara F, Sourjik V, Eils R and König R: Machine learning based analyses on metabolic networks supports high-throughput knockout screens. BMC Syst Biol 2: 67, 2008.

36. Zhang Z, Rui W, Wang ZC, Liu DX and Du L: Anti-proliferation and anti-metastasis effect of barbaloin in non-small cell lung cancer via inactivating p38MAPK/Cdc25B/Hsp27 pathway. Oncol Rep 38: 1172-1180, 2017.
37. Mirzaei H, Shakeri A, Rashidi B, Jalili A, Banikazemi Z and Sahebkar A: Phytosomal curcumin: A review of pharmacokinetic, experimental and clinical studies. Biomed Pharmacother 85: 102-112, 2017.
38. Hoehle SI, Pfeiffer E, Sólyom AM and Metzler M: Metabolism of curcuminoids in tissue slices and subcellular fractions from rat liver. J Agric Food Chem 54: 756-764, 2006.
39. Vareed SK, Kakarala M, Ruffin MT, Crowell JA, Normolle DP, Djuric Z and Brenner DE: Pharmacokinetics of curcumin conjugate metabolites in healthy human subjects. Cancer Epidemiol Biomarkers Prev 17: 1411-1417, 2008.
40. Lu CC, Chen HP, Chiang JH, Jin YA, Kuo SC, Wu TS, Hour MJ, Yang JS and Chiu YJ: Quinazoline analog HMJ-30 inhibits angiogenesis: Involvement of endothelial cell apoptosis through ROS-JNK-mediated death receptor 5 signaling. Oncol Rep 32: 597-606, 2014.
41. Shimokawa Ki K, Katayama M, Matsuda Y, Takahashi H, Hara I, Sato H and Kaneko S: Matrix metalloproteinase (MMP)-2 and MMP-9 activities in human seminal plasma. Mol Hum Reprod 8: 32-36, 2002.
42. Nishio K, Motozawa K, Omagari D, Gojoubori T, Ikeda T, Asano M and Gionhaku N: Comparison of MMP2 and MMP9 expression levels between primary and metastatic regions of oral squamous cell carcinoma. J Oral Sci 58: 59-65, 2016.
43. Fan L, Zhang Y, Zhou Q, Liu Y, Gong B, Lü J, Zhu H, Zhu G, Xu Y and Huang G: Casticin inhibits breast cancer cell migration and invasion by down-regulation of PI3K/Akt signaling pathway. Biosci Rep 38: BSR20180738, 2018.
44. Palange AL, Di Mascolo D, Singh J, De Franceschi MS, Carallo C, Gnasso A and Decuzzi P: Modulating the vascular behavior of metastatic breast cancer cells by curcumin treatment. Front Oncol 2: 161, 2012.
45. Coker-Gurkan A, Celik M, Ugur M, Arisan ED, Obakan-Yerlikaya P, Durdu ZB and Palavan-Unsal N: Curcumin inhibits autocrine growth hormone-mediated invasion and metastasis by targeting NF-κB signaling and polyamine metabolism in breast cancer cells. Amino Acids 50: 1045-1069, 2018.
46. Gallardo M and Calaf GM: Curcumin inhibits invasive capabilities through epithelial mesenchymal transition in breast cancer cell lines. Int J Oncol 49: 1019-1027, 2016.
47. Hu C, Li M, Guo T, Wang S, Huang W, Yang K, Liao Z, Wang J, Zhang F and Wang H: Anti-metastasis activity of curcumin against breast cancer via the inhibition of stem cell-like properties and EMT. Phytomedicine 58: 152740, 2019.
48. Guan F, Ding Y, Zhang Y, Zhou Y, Li M and Wang C: Curcumin suppresses proliferation and migration of MDA-MB-231 breast cancer cells through autophagy-dependent Akt degradation. PLoS One 11: e0146553, 2016.
49. Turro E, Astle WJ, Megy K, Gräf S, Greene D, Shamardina O, Allen HL, Sanchis-Juan A, Frontini M, Thys C, *et al*: Whole-genome sequencing of patients with rare diseases in a national health system. Nature 583: 96-102, 2020.
50. Collado-Torres L, Nellore A, Kammers K, Ellis SE, Taub MA, Hansen KD, Jaffe AE, Langmead B and Leek JT: Reproducible RNA-seq analysis using recount2. Nat Biotechnol 35: 319-321, 2017.
51. Vamathevan J, Clark D, Czodrowski P, Dunham I, Ferran E, Lee G, Li B, Madabhushi A, Shah P, Spitzer M and Zhao S: Applications of machine learning in drug discovery and development. Nat Rev Drug Discov 18: 463-477, 2019.
52. Zhou W, Yui MA, Williams BA, Yun J, Wold BJ, Cai L and Rothenberg EV: Single-cell analysis reveals regulatory gene expression dynamics leading to lineage commitment in early T cell development. Cell Syst 9: 321-337. e9, 2019.
53. Byrne A, Cole C, Volden R and Vollmers C: Realizing the potential of full-length transcriptome sequencing. Philos Trans R Soc Lond B Biol Sci 374: 20190097, 2019.
54. Zhang Y, Moerkens M, Ramaiahgari S, de Bont H, Price L, Meerman J and van de Water B: Elevated insulin-like growth factor 1 receptor signaling induces antiestrogen resistance through the MAPK/ERK and PI3K/Akt signaling routes. Breast Cancer Res 13: R52, 2011.
55. Lin CC, Chen KB, Tsai CH, Tsai FJ, Huang CY, Tang CH, Yang JS, Hsu YM, Peng SF and Chung JG: Casticin inhibits human prostate cancer DU 145 cell migration and invasion via Ras/Akt/NF-κB signaling pathways. J Food Biochem 43: e12902, 2019.
56. Chen WC, Lai YA, Lin YC, Ma JW, Huang LF, Yang NS, Ho CT, Kuo SC and Way TD: Curcumin suppresses doxorubicin-induced epithelial-mesenchymal transition via the inhibition of TGF-β and PI3K/AKT signaling pathways in triple-negative breast cancer cells. J Agric Food Chem 61: 11817-11824, 2013.
57. Berrak Ö, Akkoç Y, Arısan ED, Çoker-Gürkan A, Obakan-Yerlikaya P and Palavan-Ünsal N: The inhibition of PI3K and NFκB promoted curcumin-induced cell cycle arrest at G2/M via altering polyamine metabolism in Bcl-2 overexpressing MCF-7 breast cancer cells. Biomed Pharmacother 77: 150-160, 2016.
58. Fusté NP, Fernández-Hernández R, Cemeli T, Mirantes C, Pedraza N, Rafel M, Torres-Rosell J, Colomina N, Ferrezuelo F, Dolcet X and Garí E: Cytoplasmic cyclin D1 regulates cell invasion and metastasis through the phosphorylation of paxillin. Nat Commun 7: 11581, 2016.
59. Maldonado MDM and Dharmawardhane S: Targeting rac and Cdc42 GTPases in cancer. Cancer Res 78: 3101-3111, 2018.
60. Stengel K and Zheng Y: Cdc42 in oncogenic transformation, invasion, and tumorigenesis. Cell Signal 23: 1415-1423, 2011.
61. Huang TY, Peng SF, Huang YP, Tsai CH, Tsai FJ, Huang CY, Tang CH, Yang JS, Hsu YM, Yin MC, *et al*: Combinational treatment of all-trans retinoic acid (ATRA) and bisdemethoxycurcumin (BDMC)-induced apoptosis in liver cancer Hep3B cells. J Food Biochem 44: e13122, 2020.
62. Body S, Esteve-Arenys A, Miloudi H, Recasens-Zorzo C, Tchakarska G, Moros A, Bustany S, Vidal-Crespo A, Rodriguez V, Lavigne R, *et al*: Cytoplasmic cyclin D1 controls the migration and invasiveness of mantle lymphoma cells. Sci Rep 7: 13946, 2017.
63. Chen K, Jiao X, Ashton A, Di Rocco A, Pestell TG, Sun Y, Zhao J, Casimiro MC, Li Z, Lisanti MP, *et al*: The membrane-associated form of cyclin D1 enhances cellular invasion. Oncogenesis 9: 83, 2020.
64. Du DS, Yang XZ, Wang Q, Dai WJ, Kuai WX, Liu YL, Chu D and Tang XJ: Effects of CDC42 on the proliferation and invasion of gastric cancer cells. Mol Med Rep 13: 550-554, 2016.